Corn silk extract–based solid-state biopolymer electrolyte and its application to electrochemical storage devices

Article *in* Ionics · April 2022

DOI: 10.1007/s11581-021-04415-0

CITATIONS
8

READS
945

5 authors, including:

Suvarnna Kumaresan
PSGR Krishnammal College for Women
7 PUBLICATIONS **16** CITATIONS
SEE PROFILE

Dr Jone Kirubavathy Suyambulingam
PSGR Krishnammal College for Women TamilNadu India
32 PUBLICATIONS **306** CITATIONS
SEE PROFILE

Selvasekarapandian Subramanian
Materials Research Center, Coimbatore-641045 India
384 PUBLICATIONS **9,375** CITATIONS
SEE PROFILE

Vengadesh Krishna M
Bharathiar University
21 PUBLICATIONS **164** CITATIONS
SEE PROFILE

Ionics
https://doi.org/10.1007/s11581-021-04415-0

ORIGINAL PAPER

Corn silk extract–based solid-state biopolymer electrolyte and its application to electrochemical storage devices

K. Suvarnna[1,2] · S. Jone Kirubavathy[1] · S. Selvasekarapandian[2,3] · M. Vengadesh Krishna[2] · Mangalam Ramaswamy[4]

Received: 19 September 2021 / Revised: 14 December 2021 / Accepted: 15 December 2021

Abstract

A solid-state biopolymer electrolyte was prepared from the biomaterial Corn Silk Extract (CSE) by blending with polyvinyl alcohol and different concentration of $MgCl_2$ by opting solution casting technique. The maximum ionic conductivity of 1.74×10^{-5} Scm^{-1} for the blend pure biopolymer (0.9 g CSE + 1 g PVA) and 1.28×10^{-3} Scm^{-1} for the biopolymer electrolyte was obtained from the AC Impedance analysis. The obtained biopolymer electrolyte is characterized by Fourier transform infrared spectroscopy to look into the complex formation of the biopolymer blend and the salt. The maximum amorphous nature has been observed for 0.9 g CSE + 1 g PVA + 0.45wt% $MgCl_2$ by the XRD technique. Glass transition temperature of the biopolymer electrolyte was found by the differential scanning calorimetry (DSC) process. The electrochemical potential window of the biopolymer electrolyte with maximum conductivity is obtained as 2.65 V in linear sweep voltammetry (LSV). The transference number is calculated from Wagner's and Evan's polarization techniques. A primary Mg-ion battery is constructed with an open-circuit voltage of 1.95 V at room temperature.

Keywords Corn silk extract · Biopolymer · AC impedance analysis · Primary magnesium battery

Introduction

The study of biopolymer electrolytes in energy devices is one of the potential fields with a plethora of applications to be explored. Electrochemical energy storage devices are considered to be one of the productive ways of storing energy in an eco-friendly approach. To produce clean energy storage devices, the focus is turned on the biodegradable solid biopolymers due to their low cost, eco-friendly, and bio-degradable nature. A wide variety of biopolymers, for instance, pectin, agar–agar, dextrin, cellulose acetate, are utilized for the electrolyte preparation [1–7].

Corn silk, a biomaterial, is one of the byproducts of Corn (Zea Mays). Corn silk (biowaste) extract contains abundant hydroxyl groups in its flavonoids, polysaccharidic [8, 9] network which can act as the coordination site for the cation of any salt. Corn silk extract comprises dietary fiber, alkaloids, steroids, and also phenolics such as flavonoids [10–13]. They also possess lipids, carbohydrates, proteins, vitamins, minerals, and volatile oils [14]. They have multiple pharmacological activities such as anti-tumor, antioxidant, anti-obesity, anti-inflammatory, and many other activities due to the presence of polysaccharide [15] content and also used in the treatment of hypertension, kidney stones, and even prostatitis [16]. Due to this structural composition of the corn silk (Fig. 1) and also from the GC–MS spectroscopy analysis, the extract has been chosen as an ideal biomaterial. Some of the compounds of corn silk extract which may be responsible for their conducting nature are melezitose, 2-deoxy-D-galactose, 3,3-diethoxy 1-propanol, dihydroartemisinin, and 1-docosene.

In the present study, corn silk, a biowaste is selected for the preparation of solid biopolymer electrolyte, since the various components of corn silk contain a good amount of –OH groups

✉ S. Jone Kirubavathy
jonekiruba@psgrkcw.ac.in

✉ S. Selvasekarapandian
sekarapandian@rediffmail.com

1 PSGR Krishnammal College for Women, Tamil Nadu, Coimbatore 641004, India

2 Materials Research Center, Tamil Nadu, Coimbatore 641045, India

3 Department of Physics, Bharathiar University, Tamil Nadu, Coimbatore 641046, India

4 PSG Institute of Technology and Applied Research, Tamil Nadu, Coimbatore 641062, India

Published online: 24 January 2022

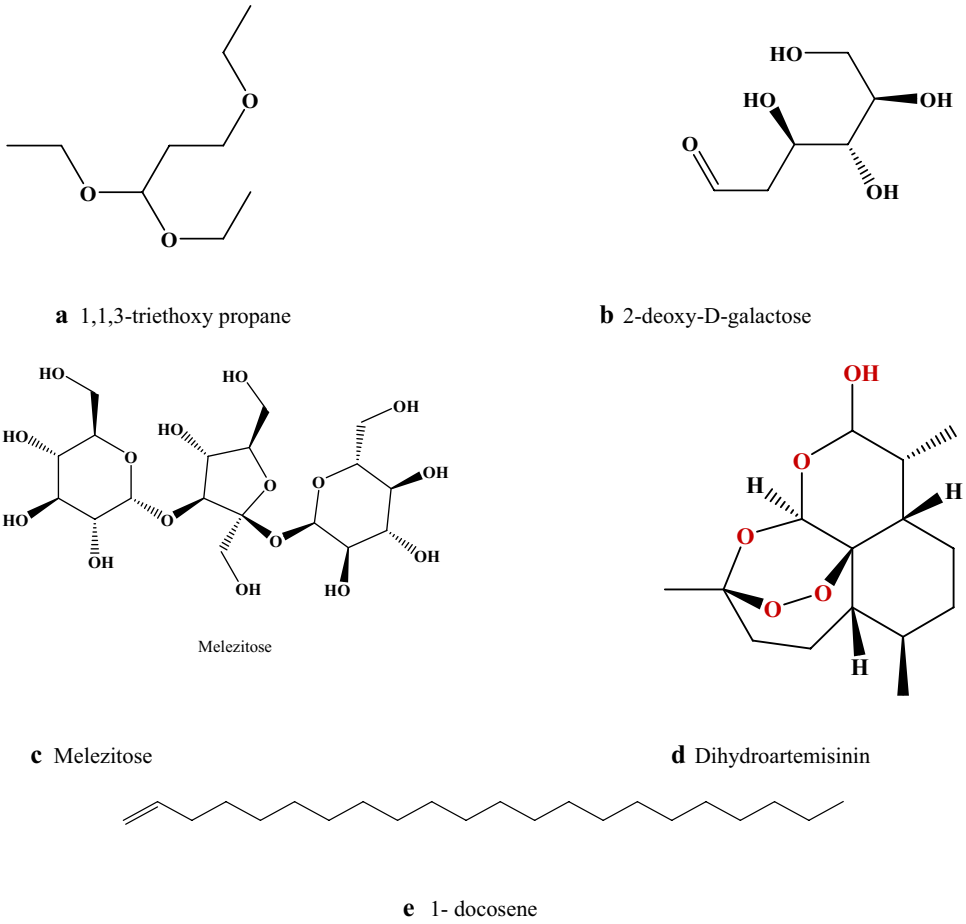

Fig. 1 Components present in corn silk extract

[15, 17, 18]. This is the novelty of the system. Only a very few works have been reported using corn silk. Corn silk has been used as carbon for electrode material [19, 20]. The corn silk extract (biomaterial) does not have enough film-forming capacity, so it has been blended with polyvinyl alcohol (PVA) to prepare a biopolymer electrolyte. PVA is having a good film-forming capacity and can be blended with any material easily. This paper mainly focuses on the development of an Mg-ion battery with corn silk extract (CSE) and PVA.

Nowadays, in devices like cell phones and laptops, lithium-ion batteries have been mostly used. But lithium-ion batteries are relatively costly, form dendrites, and also are considered less safe for handling due to their explosive nature. Henceforth, the researchers are working to develop other types of batteries. Among them, magnesium is a good choice because it is abundant in the earth's crust compared to lithium. Magnesium also lacks dendrite formation which overcomes the performance challenges. It is also easy to handle and low cost and also has a high melting point (649 °C). The divalent property of Mg^{2+} provides them a high theoretical volumetric capacity of 3832 mAh cm^{-3}, compared to Li^{+} of 2062 mAh cm^{-3} [21]. The main advantage of employing magnesium for energy storage application includes chemical and electrochemical stability [22] of magnesium metal anode and its high coulombic efficiency. Because of all the above facts, magnesium is considered the best alternative for next-level battery applications.

From the broad literature survey, the design of a new magnesium-ion-conducting biopolymer electrolyte with sufficient stability and reversibility has been explored. Manjula Devi et al. produced a solid blend polymer electrolyte using polyvinyl alcohol and polyacrylonitrile with 0.5 mm% of $MgCl_2$ [23]. Sangeetha et al. fabricated a primary magnesium battery using a biopolymer electrolyte κ-carrageenan and $MgCl_2$ as dopant [24]. Chitosan-based polymer electrolyte doped with $MgCl_2$ was carried out by H. Hamsan et al. [25]. Magnesium-ion-conducting biopolymer electrolyte was prepared by M. Mahalakshmi et al., using cellulose acetate with magnesium perchlorate [26]. P. Perumal et al. [27] used a biomaterial, tamarind seed polysaccharide to prepare a primary Mg-ion battery using magnesium perchlorate. Literature studies reveal that no work has been carried out with corn silk extract in this field of energy storage.

The main objective is to develop the Mg-ion-conducting solid-state biopolymer electrolyte using CSE, PVA, and $MgCl_2$ by solution casting approach. The prepared membrane has been characterized by AC impedance analysis, X-ray diffraction (XRD), Fourier transform infrared

spectroscopy (FTIR), differential scanning calorimetry (DSC), linear sweep voltammetry (LSV), transference number, and primary battery analysis.

Experimental

Methods and materials

Polyvinyl alcohol (PVA) (mol.wt – 85,000—1,24,000, Sigma-Aldrich) and magnesium chloride ($MgCl_2$. $6H_2O$) (mol.wt – 203.30, Spectrum) are purchased and used as such. Corn silk obtained from the local farm is used as the starting material. Double-distilled water and ethanol are used as solvents.

Preparation of corn silk extract (CSE)

The corn silk extract is prepared from 8 g of corn silk. At first, the corn silk is cut into pieces. It is then washed well with distilled water and then with ethanol. Thirty milliliters of ethanol is added to the beaker containing corn silk. The solution is then heated to about 40 °C for almost 4 h with mechanical stirring and then allowed to cool to room temperature. The extract thus obtained is brown and is now filtered and stored in an air-tight container at 4 °C which can be used for up to 6 months.

The prepared biomaterial CSE lacks a free film-forming tendency, and hence it is blended with PVA, due to its non-toxic, water-soluble, eco-friendly nature, and also its good film-forming nature. It is to be noted that the ionic conductivity of the semicrystalline, pure PVA is 2.5×10^{-10} Scm^{-1} [28] which has been considerably increased to 1.747×10^{-5} Scm^{-1} when the biomaterial is blended with 1 g PVA. This enunciates the fact that the biomaterial CSE has a significant contribution to the conductivity of the biopolymer electrolyte.

Gas chromatography–mass spectrometry analysis

Instrumentation

The Clarus SQ 8C Gas Chromatography-Mass Spectrometer from PerkinElmer was engaged for analysis. The instrument was set as follows: injector port temperature set as 250 °C, source kept at 220 °C. The oven temperature-programmed as available: 75 °C for 2 min, 150 °C @ 10 °C/min, up to 250 °C @ 10 °C/min. The split ratio was set as1:12 and the injector used was splitless mode. The DB-5 MS capillary standard non-polar column was used whose dimensions were 0.25 mm OD×0.25 µm ID×30-m length procured from Agilent Co., USA. Helium was used as the carrier gas at 1 ml/min. The MS was set to scan from 50 to 550 Da. The source was maintained at 220 °C and $4.5e^{-6}$ m torr vacuum pressure. The ionization energy was −70 eV. The MS was also having an inbuilt pre-filter which reduced the neutral particles. The data system has inbuilt libraries for searching and matching the spectrum. NIST MS Search 2.2v contains more than five lakh references.

Identification of compounds

Interpretation of mass spectrum of GC–MS was done using the database of National Institute Standard and Technology (NIST14). The spectrum of the known component was compared with the spectrum of the known components stored in the inbuilt library. The GC–MS analysis of the ethanolic extract of corn silk was performed. This analysis was carried out to determine the possible chemical components in the ethanolic extract of corn silk. The GC–MS analysis shows that the extract mainly contained the following compounds like melezitose, 3,3-diethoxy 1-propanol, 1-docosene, dodecane, pentaborane. The GC–MS chromatogram of the compounds is listed in the Appendix.

Preparation of the biopolymer film and biopolymer electrolyte

The biopolymer membrane has been prepared as in Fig. 2, using CSE and PVA. One gram of PVA is dissolved in 20 ml of double-distilled water to get a homogenous solution. CSE of different quantities (0.5 g, 0.75 g, 0.9 g) has been added to the PVA solution and is stirred for 48 h. The resulting solution is vacuum dried at 80 °C to remove the solvent After 48 h, free-standing membranes are obtained. The prepared biopolymer film with different concentrations of CSE was optimized from their conductivity values in Table 1 and 0.9 g CSE + 1 g PVA is chosen as the pure biopolymer. Later, addition of $MgCl_2$ in different weight percentage as 0.3wt% (0.6099 g), 0.4wt% (0.8132 g), 0.45wt% (0.91485 g), 0.5wt% (1.0165 g) is added to the optimized pure blend (0.9 g CSE + 1 g PVA). The solution is then again blended for about 24 h thus ensuring the proper mixing of the salt into the polymer, after which the solution is cast into the polypropylene Petri dishes and they are vacuum dried at 80 °C for 12 h for the removal of moisture content. Then, the prepared solid biopolymer electrolyte is stored in a desiccator for further analysis.

Characterization techniques

The amorphous/crystalline nature of the prepared membrane has been studied using XRD (Rigaku Ultima IV diffractometer with Cu–Kα radiation in the range of $2\theta = 10$ to 80° at room temperature). Complex formation between the biopolymer and the salt has been studied using FT-IR (SHIMADZU–IR Affinity-1 Spectrometer) in the frequency range 400 to 4000 cm^{-1} with the resolution of 1 cm^{-1}. Glass transition temperature (T_g) of the biopolymer electrolyte has been studied using DSC technique (DSC Q20 V24.11 Build 124 under nitrogen atmosphere in the temperature range from 20 to 200 °C at the heating rate of 10 °C/min). The electrochemical potential window is studied using linear

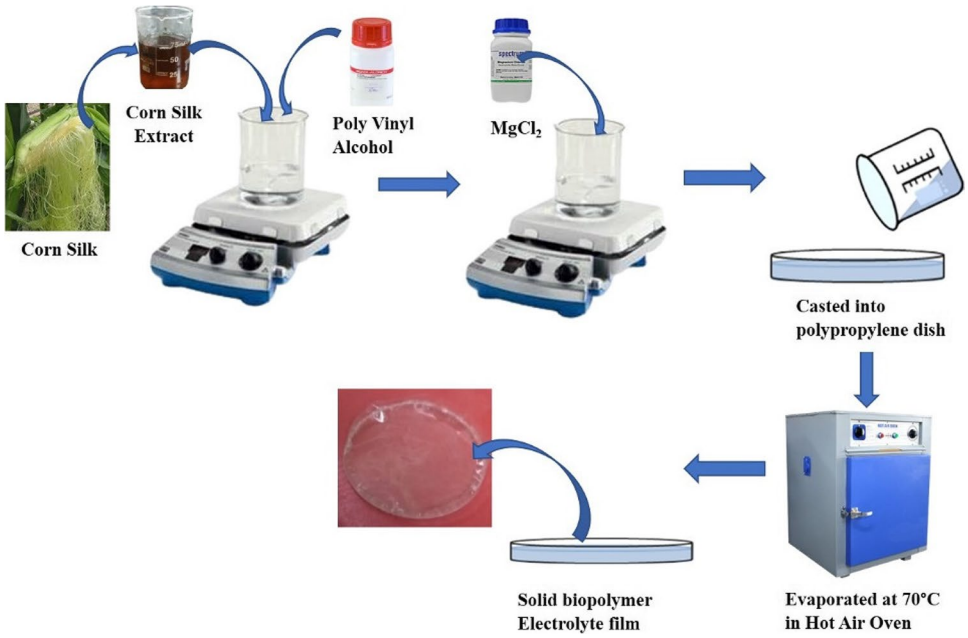

Fig. 2 Scheme for preparation of solid biopolymer electrolyte

Table 1 Ionic conductivity (σ) values of the biopolymer at 303 K

Composition	σ (S cm^{-1})	R_b (Ohms)
0.5 g CSE + 1 g PVA	5.911×10^{-8}	64,708.94
0.75 g CSE + 1 g PVA	4.649×10^{-7}	21,071.82
0.9 g CSE + 1 g PVA	1.747×10^{-5}	220.13
1 g CSE + 1 g PVA	5.791×10^{-7}	7440.69

sweep voltammetry, to estimate the exact working potential of the prepared biopolymer electrolytes. The measurement was performed by Biologic VSP – 300, with a two-electrode system at the scan rate of 1mVs^{-1} in the 0–5-V potential range at room temperature. AC impedance analysis has been measured using the HIOKI-IM 3532 LCR meter Hi-tester in the frequency range of about 42 to 1 MHz at room temperature. Wagner's and Evan's methods have been used to study the transfer number measurements. A primary Magnesium battery is constructed by employing the high-conducting $MgCl_2$-doped biopolymer film. Magnesium is taken as the anode and cathode is prepared by grinding the MnO_2:graphite:biopolymer electrolyte in the ratio (3:1:0.5) and pelletizing them.

Results and discussion

XRD studies

XRD measurements of the biopolymer electrolyte have been made to determine the amorphous/crystalline nature of the biopolymer electrolyte. Figure 3 represents the XRD pattern of pure CSE, pure PVA, and pure biopolymer (0.9 g CSE + 1 g PVA) and Fig. 4 shows the XRD pattern of magnesium chloride salt. The liquid XRD pattern of corn silk extract contains a broad peak at 16.3°, 31.8°, and 40.0° which may be due to the components of corn silk extract. When CSE is blended with PVA, peaks at 19.6°, 31.5°, and 44.4° are observed. The peak observed for CSE is not seen when it is blended with PVA. The peak observed for CSE at 31.8° and 40.0° might have shifted to 31.5° and 44.4°. The peak at 19.6° is due to PVA [23]. The peak at 16.3° would have merged with the peak at 19.6° in the pure biopolymer membrane (0.9 g CSE + 1 g PVA). Figure 5b, c, d, and e show the XRD pattern for the composition 0.9 g CSE + 1 g PVA + 0.3wt% $MgCl_2$, 0.9 g CSE + 1 g PVA + 0.4wt% $MgCl_2$, 0.9 g CSE + 1 g PVA + 0.45wt% $MgCl_2$, and 0.9 g CSE + 1 g PVA + 0.5wt% $MgCl_2$ respectively.

It is observed from the curve in Fig. 5b that the peaks at 19.6° get shifted to 21.7° and it has been broadened. The peaks viewed at 31.5° and 44.4° disappeared due to the addition of 0.3wt% of $MgCl_2$. It is also noted that as the salt concentration increases to 0.4wt% of $MgCl_2$, the peak at 19.6° is still more broadened. Meanwhile, as the concentration increases to 0.45wt% of $MgCl_2$, it is observed from Fig. 5d that the intensity of the peak at 19.6° is still decreased. The increase in the broadening nature and decrease in the intensity lead to the conclusion that the amorphous nature of the biopolymer electrolyte has much increased. The increase in the amorphous nature causes a reduction in the energy barrier due to the segmental motion of the polymer electrolyte Pandi et al. [29, 30]. On further increase in concentration to 0.9 g CSE + 1 g PVA + 0.5wt% $MgCl_2$, we can observe peaks at 28.4°, 29.3°, 31.6°, 45.3°,

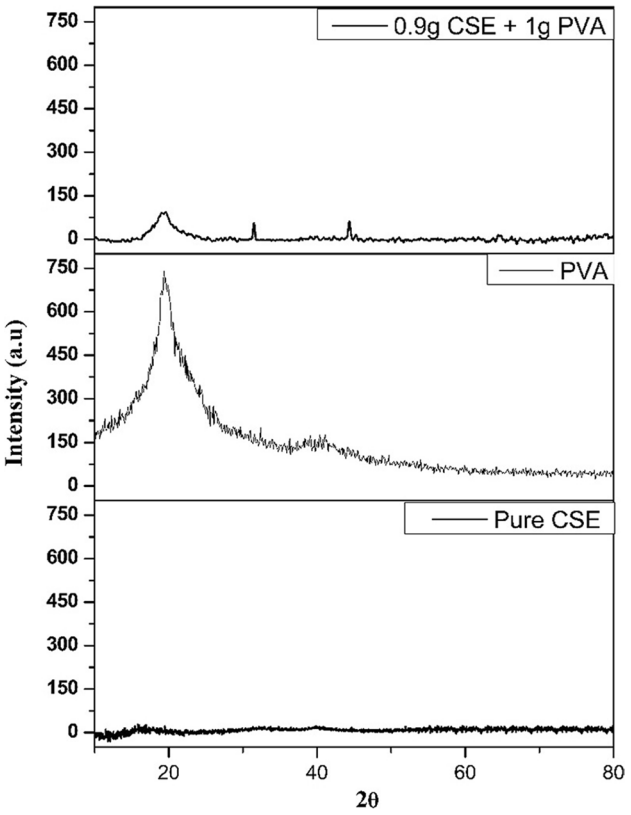

Fig. 3 XRD pattern of pure CSE, pure PVA, and pure (0.9 g CSE + 1 g PVA)

and 56.4°. The broadness of the peak at 19.6° due to PVA is decreased. The above peaks are in correspondence with the $MgCl_2$ peaks (JCPDS Number 72–1517) at $2\theta = 14.9°$, 28.2°, 30.1°, 32.1°,41.7°, 45.8°, 50°, and 52.5° given by Manjula Devi et al. [23]. This correlates with the fact of recrystallization of added $MgCl_2$ at Pure + 0.5wt%.

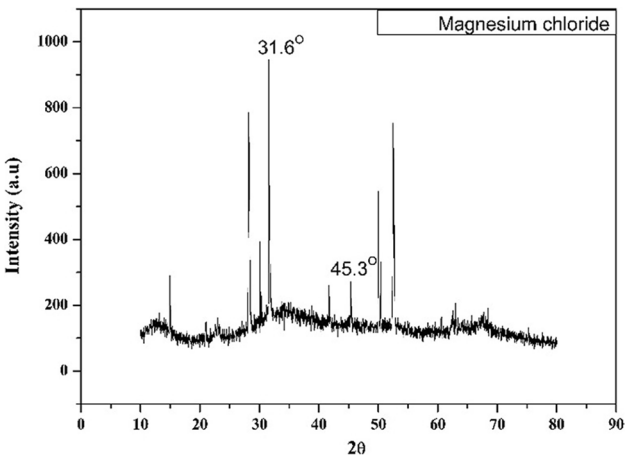

Fig. 4 XRD pattern of magnesium chloride salt

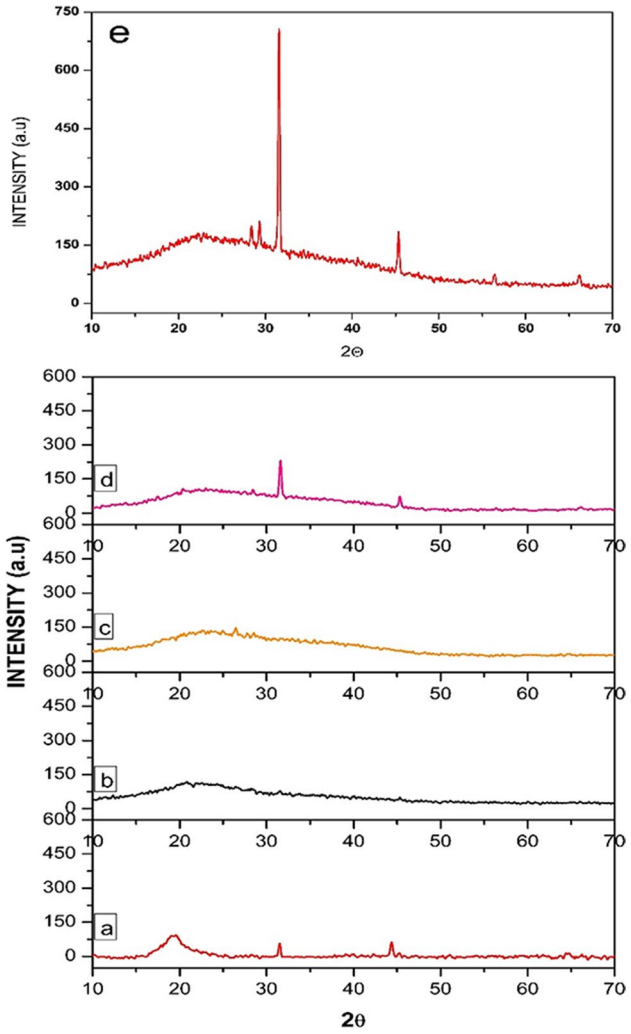

Fig. 5 XRD pattern of (**a**) pure (0.9 g CSE + 1 g PVA), (**b**) Pure + 0.3wt% $MgCl_2$, (**c**) Pure + 0.4wt% $MgCl_2$, (**d**) Pure + 0.45wt% $MgCl_2$, and (**e**) Pure + 0.5wt% $MgCl_2$

Figure 6 shows the deconvoluted graph. From the XRD deconvoluted pattern, the percentage of crystallinity is calculated using Formula 1.

$$\text{Percentage of Crystallinity} = \left(\frac{\%\text{ area under the crystalline peak}}{\text{The total area of the peak}}\right) \times 100 \quad (1)$$

As seen in the Table 2, it is observed that the percentage of crystallinity decreases as the salt concentration increases upto 0.4wt% $MgCl_2$. When we increase the salt concentration further to 0.45wt% $MgCl_2$ and 0.5wt% $MgCl_2$, the percentage of crystallinity increases. The above results show that the amorphous nature is maximum for Pure + 0.4wt% $MgCl_2$.

Fourier transform infrared (FT-IR) spectroscopy

FTIR spectra are used to examine the interactions among the atoms and the ions in the biopolymer electrolyte systems

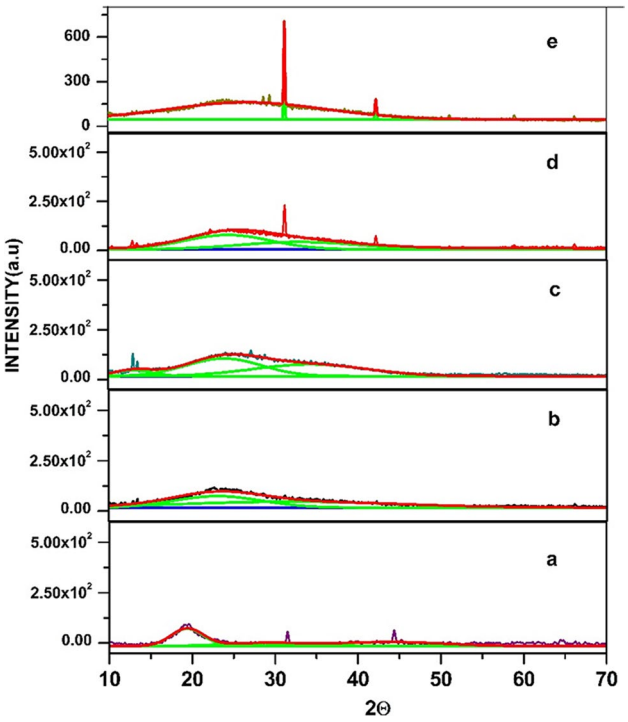

Fig. 6 Deconvoluted XRD pattern of (**a**) pure (0.9 g CSE + 1 g PVA), (**b**) Pure + 0.3wt% $MgCl_2$, (**c**) Pure + 0.4wt% $MgCl_2$, (**d**) Pure + 0.45wt% $MgCl_2$, and (**e**) Pure + 0.5wt% $MgCl_2$

Table 2 Percentage of crystallinity for the pure and pure with different concentrations of $MgCl_2$

Composition	Percentage of crystallinity
Pure (0.9 g CSE + 1 g PVA)	32.19
Pure + 0.3wt% $MgCl_2$	11.06
Pure + 0.4wt% $MgCl_2$	10.24
Pure + 0.45wt% $MgCl_2$	13.15
Pure + 0.5wt% $MgCl_2$	16.56

(Table 3). Figure 7 represents the FTIR for CSE, pure biopolymer (0.9 g CSE + 1 g PVA) and the biopolymer electrolytes 0.9 g CSE + 1 g PVA + 0.3wt% $MgCl_2$, 0.9 g CSE + 1 g PVA + 0.4wt% $MgCl_2$, 0.9 g CSE + 1 g PVA + 0.45wt% $MgCl_2$, and 0.9 g CSE + 1 g PVA + 0.5wt% $MgCl_2$ respectively. FTIR for pure PVA is given by Polu et al. [31].

A broad peak at 3344 cm^{-1} observed in Fig. 7a is assigned to the stretching vibrations of the hydroxy group with strong inter and intramolecular hydrogen bonding. This peak noticed at 3334 cm^{-1} in Fig. 7a for pure biopolymer is more broad and intense in Fig. 7b to e. This confirms the uniform blending of the CSE with PVA. When 1 g PVA is added to 0.9 g CSE, it is observed that the peak at 3334 cm^{-1} is a little bit broad due to the presence of the OH group in PVA. When the salt is added, the Mg^{2+} ion interacts with the oxygen atom of the OH group. So it becomes broader. An absorption peak at 2958 cm^{-1} corresponding to asymmetric – CH stretching vibrations has been found in the pure biopolymer (0.9 g CSE + 1 g PVA) and all electrolyte systems. This peak is shifted to lower wavelengths (2928 cm^{-1}, 2921 cm^{-1}, 2935 cm^{-1}, 2925 cm^{-1}, 2923 cm^{-1}) in all biopolymer electrolyte systems. A small peak observed at 1683 cm^{-1} in Fig. 7 for CSE may be due to – OH bending vibrations of the polyhydroxy groups in the extract. A sharp peak at 1717 cm^{-1} in Fig. 7a is assigned to C = O stretching which is shifted to a lower frequency in the salt-doped systems. CH_2 bending vibrations seen in 1406 cm^{-1} in Fig. 7b for CSE are shifted to 1426 cm^{-1} for the pure biopolymer (0.9 g CSE + 1 g PVA) and shifted to higher wavenumbers as in Table 3, in the complexed systems (Fig. 7b–e). The band at 1252 cm^{-1} may be due to the – C – O group of polyols in the extract [32, 33]. This peak is due to the complete association of CSE with PVA which can be seen in all the $MgCl_2$-doped membrane systems. A sharp peak at 1052 cm^{-1} could be due to the polysaccharides in the CSE whereas the peak at 1080 cm^{-1} in Fig. 7a corresponds to the – C O stretching of the acetyl groups present

Table 3 Peak position and vibrational assignments of pure (0.9 g CSE + 1 g PVA) and Pure + different concentrations of $MgCl_2$

Assignments	CSE	Pure (0.9gCSE + 1 g PVA)	Pure + 0.3 wt% $MgCl_2$	Pure + 0.4 wt% $MgCl_2$	Pure + 0.45wt%$MgCl_2$	Pure + 0.5 wt%$MgCl_2$
–OH stretching	3344 cm^{-1}	3334 cm^{-1}	3325 cm^{-1}	3296 cm^{-1}	3323 cm^{-1}	3324 cm^{-1}
C–H stretching vibrations	2958 cm^{-1}	2928 cm^{-1}	2921 cm^{-1}	2935 cm^{-1}	2925 cm^{-1}	2923 cm^{-1}
–OH bending of polyols	1683 cm^{-1}	-	-	-	-	-
C = O and C = C	-	1717 cm^{-1}	1649 cm^{-1}	1650 cm^{-1}	1645 cm^{-1}	1645 cm^{-1}
CH_2 bending	1406 cm^{-1}	1426 cm^{-1}	1420 cm^{-1}	1421 cm^{-1}	1432 cm^{-1}	1429 cm^{-1}
C–O stretching of the acetyl group of PVA	-	1080 cm^{-1}	1089 cm^{-1}	1090 cm^{-1}	1087 cm^{-1}	1095 cm^{-1}
Ethanol	862 cm^{-1}	827 cm^{-1}	-	-	-	-

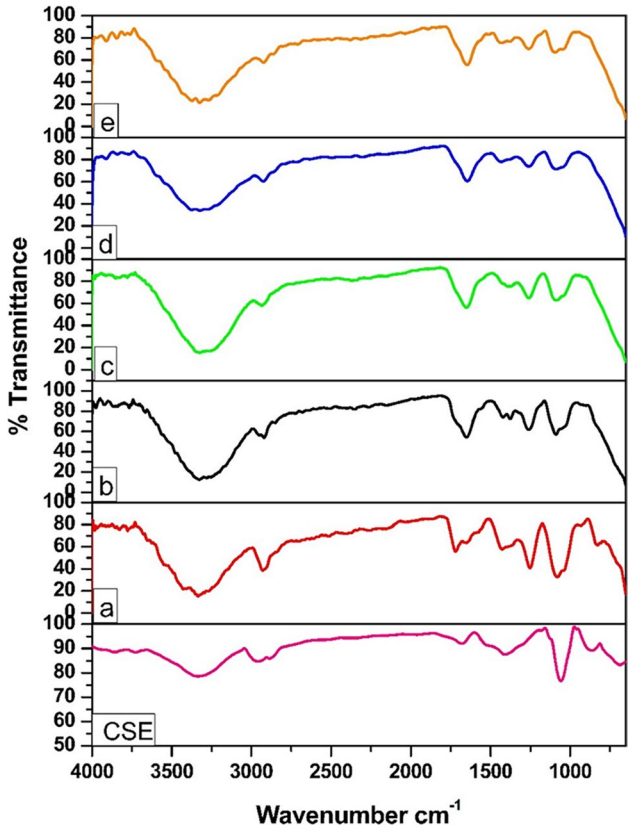

Fig. 7 FT–IR spectra of (**a**) pure (0.9 g CSE + 1 g PVA), (**b**) Pure + 0.3wt% $MgCl_2$, (**c**) Pure + 0.4wt% $MgCl_2$, (**d**) Pure + 0.45wt% $MgCl_2$, and (**e**) Pure + 0.5wt% $MgCl_2$

in the PVA backbone. This peak is shifted to higher wavenumbers from 1089–1095 cm^{-1} in all electrolyte systems. The absorption peak at 862 cm^{-1} for CSE and 827 cm^{-1} for pure biopolymer may be due to the ethanol because these peaks disappeared in all the complexed systems. Ethanol is used for the preparation of the extract which would have been evaporated during the longer blending time for the preparation of the electrolytes. Hence, from FTIR, the complex formation between CSE, PVA, and $MgCl_2$ has been confirmed.

Differential scanning calorimetry

The glass transition temperature of the prepared biopolymer electrolyte has been measured using Differential scanning calorimetry. Figure 8 represents DSC thermogram of pure CSE, pure PVA, and pure biopolymer (0.9 g CSE + 1 g PVA). Figure 9 provides the DSC thermogram of 0.9 g CSE + 1 g PVA + 0.3wt% $MgCl_2$, 0.9 g CSE + 1 g PVA + 0.4wt% $MgCl_2$, 0.9 g CSE + 1 g PVA + 0.45wt% $MgCl_2$, and 0.9 g CSE + 1 g PVA + 0.5wt% $MgCl_2$. Glass transition temperature of the biopolymer electrolyte is given in the Table 4. The glass transition temperature

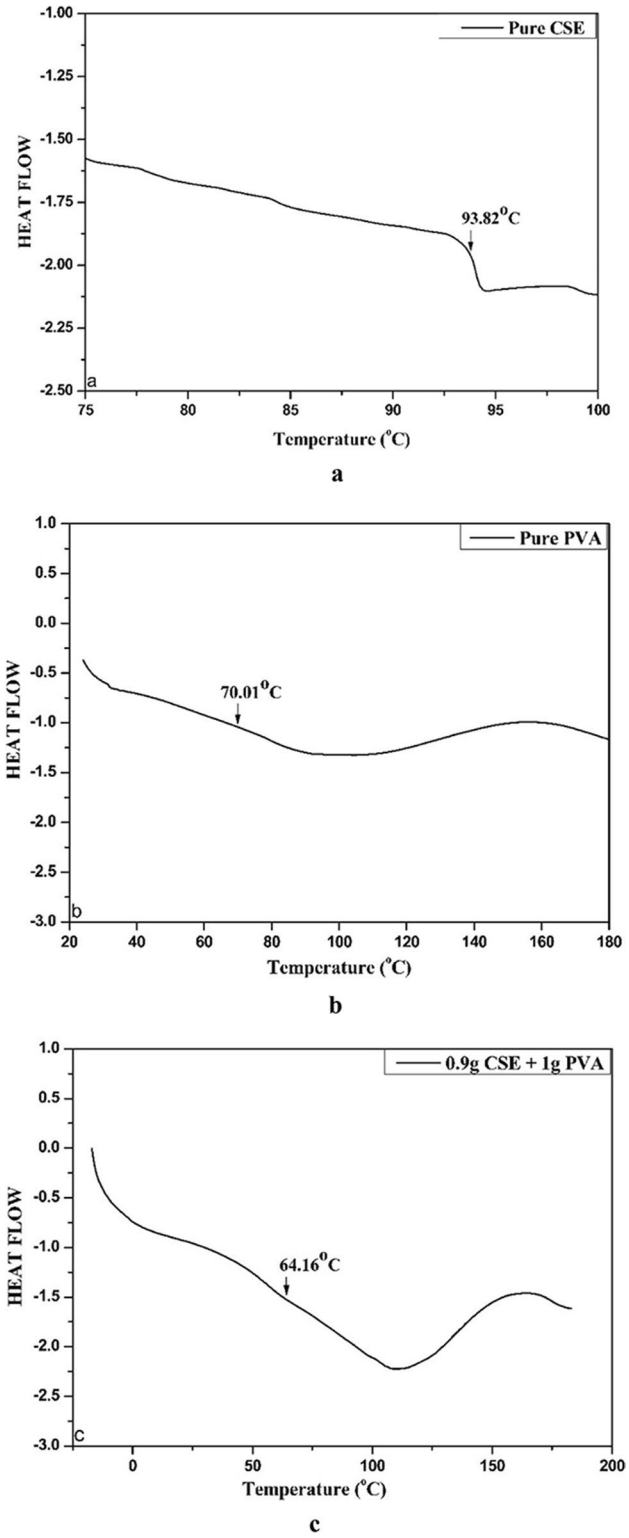

Fig. 8 (**a**, **b**, **c**) DSC thermogram of pure CSE, pure PVA, and pure (0.9 g CSE + 1 g PVA)

of pure PVA is 70.01 °C [34] and that of pure CSE is 93.82 °C. When we blend CSE with PVA, we get only one glass transition temperature. This shows the uniform

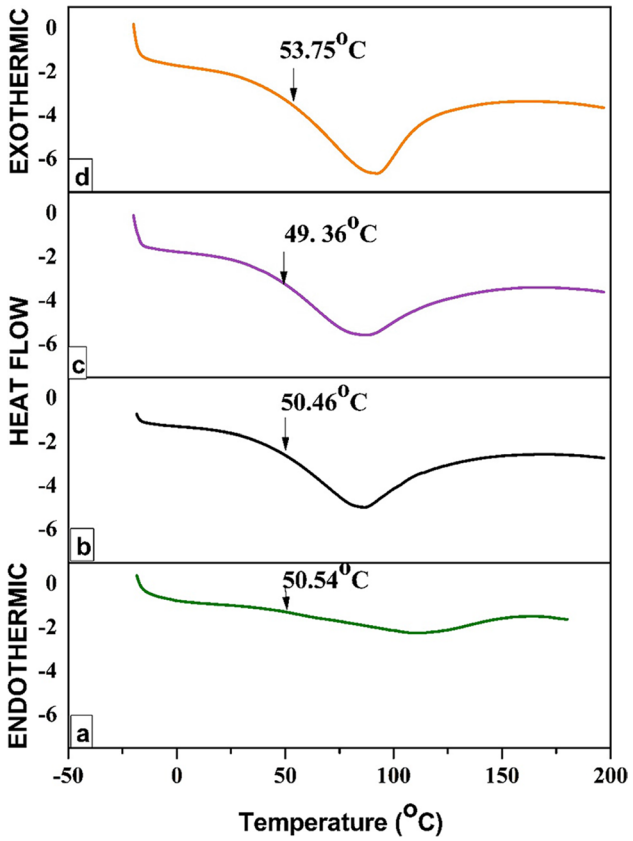

Fig. 9 DSC thermogram of (**a**) Pure + 0.3wt% $MgCl_2$, (**b**) Pure + 0.4wt% $MgCl_2$, (**c**) Pure + 0.45wt% $MgCl_2$, and (**d**) Pure + 0.5wt% $MgCl_2$

blending of the CSE with PVA. It is observed from the DSC thermogram that the T_g of 0.9 g CSE + 1 g PVA is 64.15 °C. For salt concentration 0.3wt% $MgCl_2$ added, the T_g for the membrane decreases to 50.54 °C. As the salt concentration increases to 0.9 g CSE + 1 g PVA + 0.4wt% $MgCl_2$, the glass transition temperature decreases to 50.46 °C. As on further increase of the salt concentration to 0.45wt% $MgCl_2$, the T_g value decreases to 49.36 °C. The reduced value may be due to the plasticizing effect of the salt. On the further increase of the salt concentration to 0.5wt% $MgCl_2$, T_g becomes 53.75 °C which is an indication of aggregation of salt. Similar results are observed for Manjula et al. for the polymer electrolyte film based on poly(vinyl alcohol)-poly(acrylonitrile)/$MgCl_2$ and Mahalakshmi et al. prepared a biopolymer electrolyte based on cellulose acetate with magnesium perchlorate[21, 24]. Low glass transition temperature for the 0.45wt% $MgCl_2$ denotes that the membrane is flexible. The flexible nature of the membrane leads to segmental motion.

Table 4 Glass transition temperature of pure and pure with different concentrations of $MgCl_2$

Composition	T_g
Pure CSE	93.82 °C
Pure PVA	70.01 °C
Pure (0.9 g CSE + 1 g PVA)	64.16 °C
Pure + 0.3wt% $MgCl_2$	50.54 °C
Pure + 0.4wt% $MgCl_2$	50.46 °C
Pure + 0.45wt% $MgCl_2$	49.36 °C
Pure + 0.5wt% $MgCl_2$	53.75 °C

Linear sweep voltammetry

The electrochemical stability window of the pure biopolymer and the highest conducting electrolyte (Pure + 0.45wt% $MgCl_2$) are given in Fig. 10a and 10b. Figure 10a shows that the pure biopolymer (0.9 g

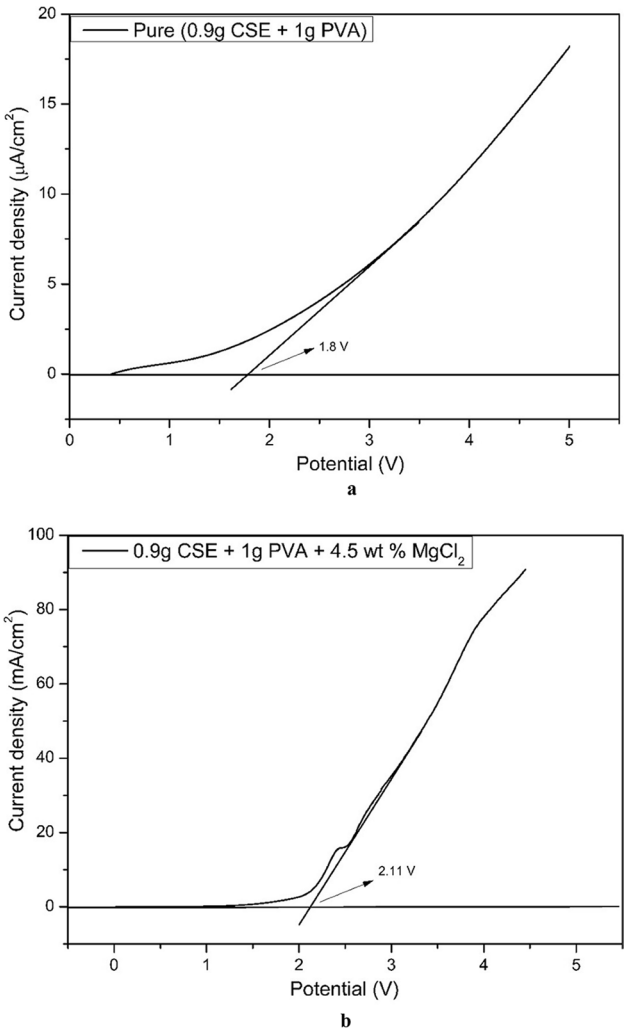

Fig. 10 (**a**, **b**) LSV plot for pure and highest Mg-ion-conducting electrolyte

CSE + 1 g PVA) has window stability up to 1.8 V which is improved in plot 10b with the addition of $MgCl_2$ to 2.11 V. The maximum electrode potential stability window of 1.83 V was obtained for Hamsan et al. [25] by using chitosan-$MgCl_2$-glycerol system and Aziz et al. obtained sharp current increase at 2.4 V for CS-glycerol-Mg(CH3COO)2-Ni system[35]. The working cell potential of the electrolyte, Pure + 0.45wt% $MgCl_2$, can be used up to 2.11 V. This is an adequate potential range for magnesium-ions in battery applications.

Transference number analysis

In transference number measurement, two kinds of approaches are adopted to establish the fact that the conductance is due to the presence of ions. One is Wagners's dc polarization technique: dc voltage 1.5 V is applied across the electrolyte of highest conducting film loaded between the stainless steel electrodes (SS/Biopolymer film/SS), in which current is observed as a function of time.

Second is Evans polarization technique: the highest conducting polymer film is selected and loaded between two magnesium electrodes (Mg/biopolymer film/Mg). Fixed dc voltage of 1.5 V is provided across the cell and the initial and final current is also noted along with impedance analysis before and after polarization. $t_{Mg}{}^{2+}$, transport number of Mg-ion, is calculated by applying the formula

$$t_{\mathrm{Mg}^{2+}}t = \frac{Is(\Delta V - RoIo)}{I_o(\Delta V - RsIs)}$$

where I_o and I_s are initial and final current, and R_o and R_s are resistance of the cell before and after polarization.

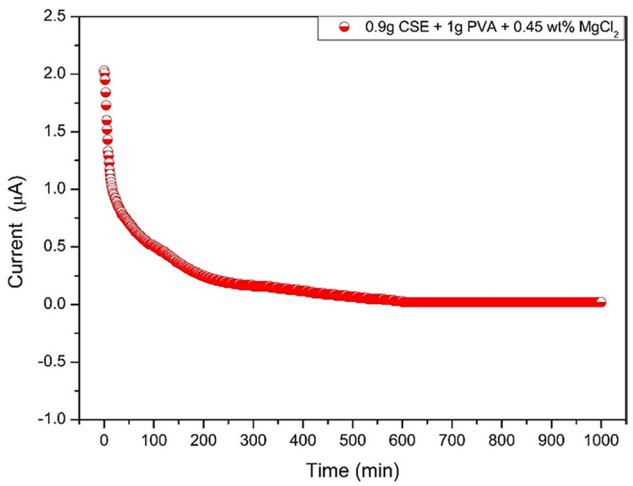

Fig. 11 Polarisation cure vs time of the cell for the highest conducting Mg-ion electrolyte

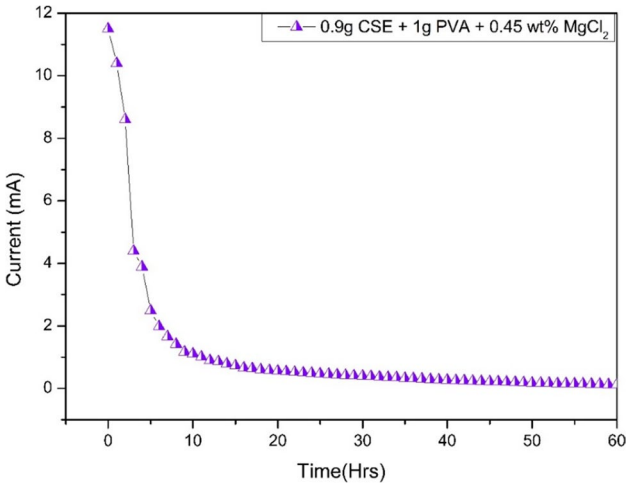

Fig. 12 DC polarization curve of the highest conducting biopolymer electrolyte containing 0.9 g CSE + 1 g PVA + 0.45wt% $MgCl_2$ with stainless steel electrode

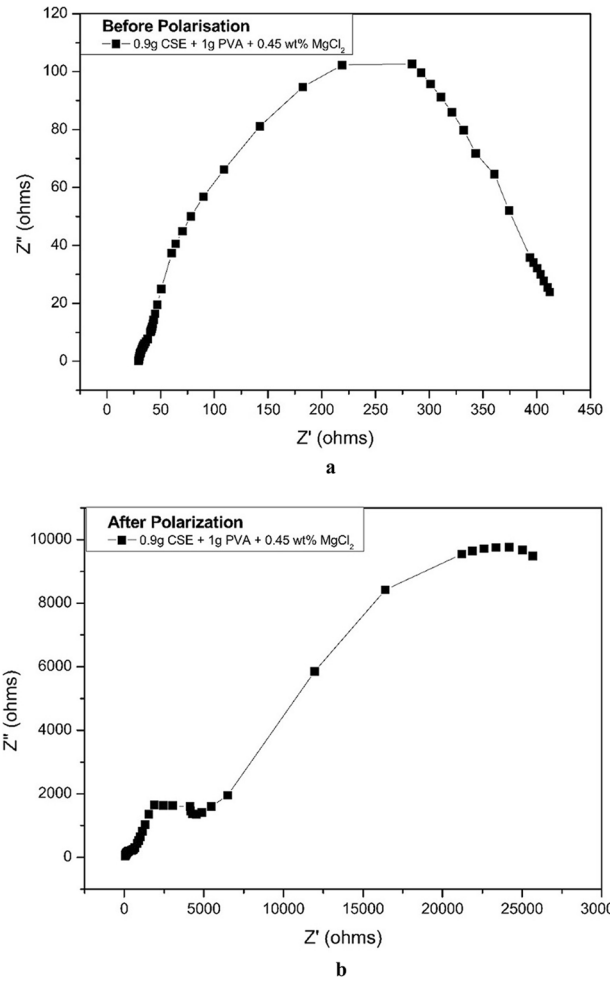

Fig. 13 (**a**, **b**) AC impedance plot for the electrolyte containing 0.9 g CSE + 1 g PVA + 0.45wt% $MgCl_2$. (a) Before polarization. (b) After polarization

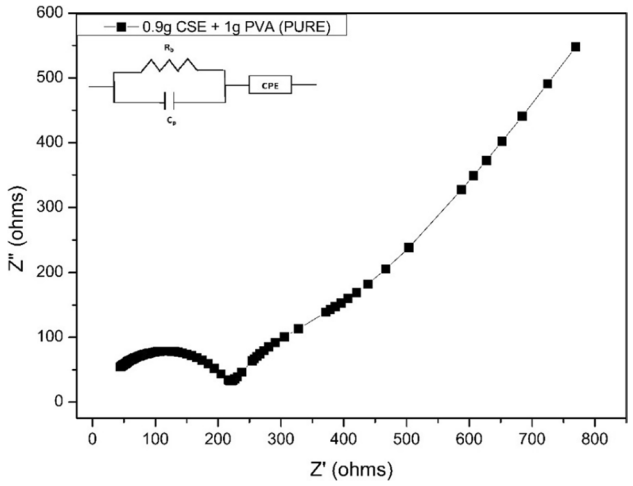

Fig. 14 Nyquist plot for the pure biopolymer (0.9 g CSE + 1 g PVA)

Wagner's polarization technique

Transference number analysis based on Wagner's polarization technique predicts whether the conducting nature of the system is either due to the ions or electrons. A constant DC potential of 1.5 V was applied to polarize SS|0.9 g CSE + 1 g PVA + 0.45wt% $MgCl_2$|SS, the cell, and the initial current is noted. Later, the current decreases and then becomes stable at a point with time, thus enabling the completion of polarization, and the final current is recorded.

The transference number can be calculated using the equation

$$t_+ = \frac{I_i - I_f}{I_i}$$

$$t_{elec} = \frac{I_f}{I_i}$$

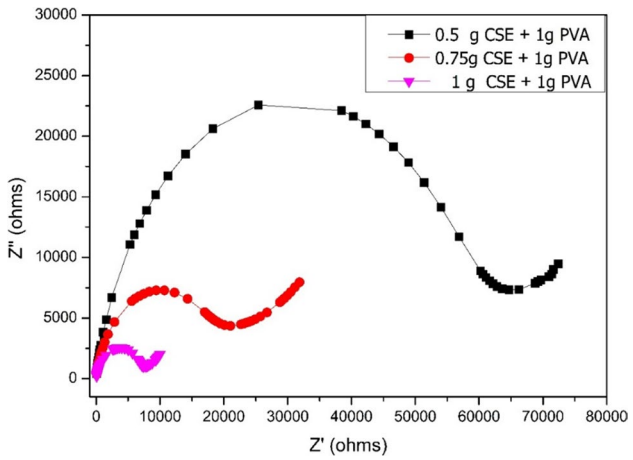

Fig. 15 Nyquist plot for the biopolymer 0.5 g CSE + 1 g PVA, 0.75 g CSE + 1 g PVA and 1 g CSE + 1 g PVA

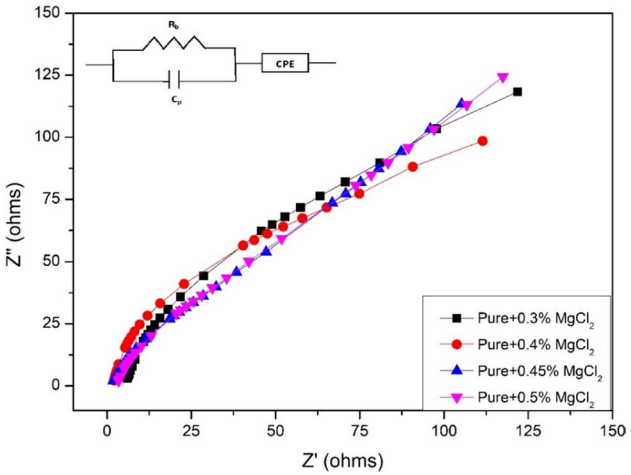

Fig. 16 Nyquist plot for the (**a**) Pure + 0.3wt% $MgCl_2$. (**b**) Pure + 0.4wt% $MgCl_2$. (**c**) Pure + 0.45wt% $MgCl_2$. (**d**) Pure + 0.5wt% $MgCl_2$

where t_+ and t_{elec} are the transference number of cation and electrons and I_i and I_f are the initial and final current respectively [6]. The transference number is obtained from the above equation as 0.99 for the highest conducting polymer matrix (Fig. 11). This confirms that the conductivity of the biopolymer system is due to the mobility of the ions and not due to electrons.

Evan's polarization technique

Evans polarization technique is used to find out the contribution of Mg-ion to conductivity. The transport number analysis of Mg^{2+} ions in the polymer matrix can be evaluated from the integration of AC and DC techniques by Evan's [36]. The initial current (I_0) and final current (I_f) were calculated from the plot in Fig. 12. Also, AC impedance spectroscopy was adopted to calculate the cell resistance R_0 and R_s before and after polarization in Fig. 13a and b. The cell resistance before and after polarization was 412.23Ω and 25,680.44Ω respectively.

The value of transference number of Mg^{2+} ions for the highest conducting electrolyte 0.9 g CSE+1 g PVA+0.45wt% $MgCl_2$ is t_+ =0.32. This value imparts significant knowledge about the

Table 5 Ionic conductivity (σ) values of the biopolymer electrolytes at 303 K

Composition	σ (S cm^{-1})	R_b (Ω)	CPE (F)	n (no units)
Pure(0.9 g CSE + 1 g PVA)	1.74×10^{-5}	220.12	2.51×10^{-8}	0.7543
Pure + 0.3wt% $MgCl_2$	3.60×10^{-4}	18.69	6.90×10^{-6}	0.8117
Pure + 0.4wt% $MgCl_2$	9.40×10^{-4}	11.93	7.30×10^{-6}	0.8236
Pure + 0.45wt% $MgCl_2$	1.28×10^{-3}	7.14	3.83×10^{-5}	0.7441
Pure + 0.5wt% $MgCl_2$	9.65×10^{-4}	7.41	2.80×10^{-5}	0.7819

contribution of Mg^{2+} ions to the conductivity of the biopolymer electrolyte. Mahalakshmi et al. have reported the value of t_+ for Mg^{2+} ions as 0.31 in their work with 40% CA:60% $Mg(ClO_4)_2$ electrolyte. Shanmugapriya et al. [37] have studied carrageenan with 0.6 g $Mg(ClO_4)_2$ electrolyte and reported t_+ as 0.313 and a similar report was provided by Ramasamy et al. [38] with 50% PVA:50% PVP and 25% $Mg(ClO_4)_2$.

AC impedance spectroscopy

Optimization of the biopolymer membrane

Figures 14 and 15 show the Nyquist plot for the pure blend, i.e., 0.9 g CSE+1 g PVA, and for the biopolymer 0.5 g CSE+1 g PVA, 0.75 g CSE+1 g PVA, and 1 g CSE+1 g PVA respectively. There is an inclined spike at the low-frequency region which is due to the constant phase element (CPE) and a depressed semicircle at the high-frequency region as given in the insert of Fig. 14. Table 1 gives the conductivity values for all the prepared compositions of biopolymers. Henceforth, 0.9 g CSE+1 g PVA is optimized as the pure biopolymer for further addition of the salt $MgCl_2$. Respective bulk resistance R_b, of each blend biopolymer electrolyte, is computed using EQ software established by B.A. Boukamp [39–41].

The ionic conductivity of the blend biopolymeric material is evaluated by AC impedance spectroscopy and estimated by using the below equation.

$$\sigma = \frac{t}{AR_b} \mathrm{Scm}^{-1}$$

where σ is the ionic conductivity, A is the contact area of the sample, t is the thickness, and R_b is the bulk resistance of the polymer membrane. From Fig. 16, it is observed that the Cole–Cole plot contains an arc with a linear spike. Their corresponding equivalent circuit is given in the insert of Fig. 16. As we increase the concentration of the salt, the value of R_b decreases. It becomes minimum for the composition (Pure+0.45wt% $MgCl_2$). On the further increase of the salt, the R_b value starts increasing.

The impedance of the constant phase element is represented by

$$Z_{CPE} = 1/Q_0(j\omega)^n$$

where Q_0 and n are the frequency-independent parameters. n varies from 0 to 1. If $n=1$, it represents a pure capacitor. If $n=0$, it represents a pure resistor. ω is the angular frequency (radians/s) and j is the imaginary number. The values of n are given in Table 5. The ionic conductivity of the blend biopolymer electrolyte with different compositions of the dopant $MgCl_2$ is also given in Table 5. Figure 17 emphasizes the fact that the ionic conductivity of the biopolymer film increases when the concentration of added $MgCl_2$ increases. But with further addition of the salt, there is a decrease in the conductivity value as observed for the composition of 0.9 g CSE+1 g PVA+0.5wt% $MgCl_2$. Maximum conductance value

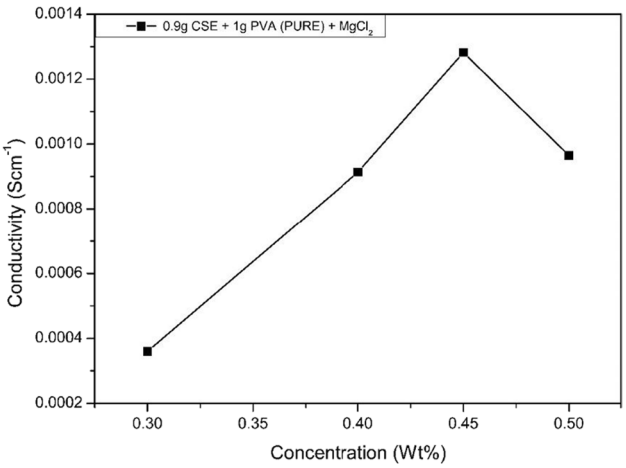

Fig. 17 Effect of concentration of magnesium chloride on the conductivity of pure biopolymer (0.9 g CSE+1 g PVA)

of 1.28×10^{-3} Scm^{-1} is observed for the composition of 0.9 g CSE+1 g PVA+0.45wt% $MgCl_2$ at room temperature. This is because of maximum charge carriers in the biopolymer electrolyte. Deconvoluted XRD pattern of the Pure+0.54wt% $MgCl_2$ indicates that it has got the crystallinity percentage as 13.15 but this percentage is higher than that of Pure+0.4wt% $MgCl_2$. However, the conductivity is maximum for Pure+0.45wt% $MgCl_2$ membrane, since it has got more charge carriers than that of Pure+0.4wt% $MgCl_2$. The segmental motion of the biopolymer membrane is due to low glass transition temperature which is also the reason for high conductivity. The decrease of conductivity for the composition 0.9 g CSE+1 g PVA+0.5wt% $MgCl_2$ is due to the formation of agglomerates [42] and also reduction of segmental motion of the biopolymer electrolyte [43]. Maximum DC ionic conductivity of 1.03×10^{-3} Scm^{-1} was obtained for M.H. Hamsan et al. for the CS: $MgCl_2$:glycerol biopolymer system. Kiruthika S S et al. [44] obtained a maximum conductivity of 1.14×10^{-3} Scm^{-1} for the biopolymer electrolyte 30 M wt% pectin: 70 M wt% $MgCl_2$. The ionic conductivity values of the present work are comparable with the above works.

Fabrication of the primary magnesium battery

The highest conducting electrolyte film is of the composition 0.9 g CSE+1 g PVA+0.45wt% $MgCl_2$, with a maximum conductivity of 1.28×10^{-3} Scm^{-1} as confirmed from the obtained results. Hence, a magnesium-ion battery is constructed with the highest conducting biopolymer membrane as the electrolyte. The cathode material used is a mixture of MnO_2 (3 g) and graphite (1 g) and biopolymer electrolyte (0.5 g) which is pelletized with a 5-ton pressure to form a pellet. Magnesium metal is chosen as the anode. Thus, the primary magnesium

battery is constructed by sandwiching the anode and cathode with the highest conducting electrolyte membrane.

The anodic and cathodic reactions may take place as given below:

At anode

$$Mg + 2(OH^-) \rightarrow Mg(OH)_2 + 2e^-$$

At cathode

$$2MnO_2 + H_2O + 2e^- \rightarrow Mn_2O_3 + 2OH^-$$

Overall reaction

$$Mg + 2MnO_2 + H_2O \rightarrow Mg(OH)_2 + Mn_2O_3$$

The oxidation potential of Mg is − 2.37 V and the reduction potential is 1.23 V. The overall theoretical cell potential E_o = 3.6 V. The open-circuit voltage of the battery was found to be 1.95 V (Fig. 19a and 19b). The discharge characteristics of the cell at room temperature when connected to an external load of 100 KΩ are depicted in Fig. 18. With a load of 100 KΩ, the current drawn was 20μA. The discharge capacity of the battery was found to be 1.2mAh. The cell potential dropped from 1.9 V and then reduces to 1.88 V and later the voltage was constant at 1.87 V up to 60 h. This decrease in voltage may be due to the polarization that occurred by the electrochemical reaction at the electrode surface (Fig. 19) [23].

Conclusions

The conductivity of the novel corn silk biopolymer (0.9 g CSE + 1 g PVA) was very fine at about 1.74×10^{-5} Scm^{-1} as predicted since the biomaterial contains a large number of hydroxy groups in their structure to increase the conductivity when blended with polyvinyl alcohol. The solid biopolymer electrolyte was developed using CSE/PVA doped with $MgCl_2$ by solution casting method. This biopolymer electrolyte was characterized by XRD, FTIR, DSC, and AC impedance spectroscopy. The amorphous nature and the complexation of the electrolyte were confirmed by XRD and FTIR techniques. The maximum conductivity of the biopolymer electrolyte about 1.28×10^{-3} Scm^{-1} was established by the EIS technique for 0.9 g CSE + 1 g PVA + 0.45 wt% $MgCl_2$. Transference number analysis reveals the fact that the conductivity of the biopolymer electrolyte was considerably due to magnesium-ions. The electrochemical potential window of the biopolymer electrolyte with maximum conductivity is obtained as 2.65 V in LSV. The primary Mg-ion battery has been constructed with the optimized high conducting membrane and an open-circuit voltage was obtained as 1.95 V at room temperature.

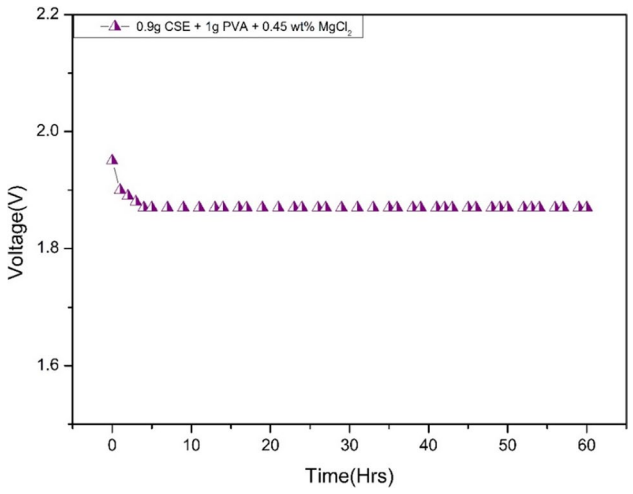

Fig. 18 Discharge curve for the cell containing the biopolymer electrolyte. 0.9 g CSE + 1 g PVA + 0.45wt% $MgCl_2$

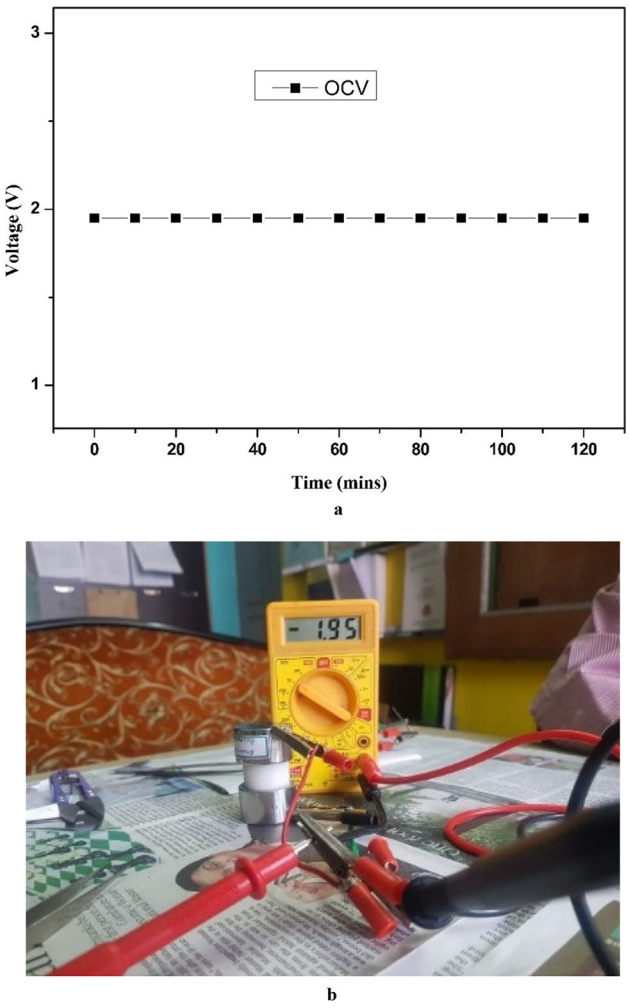

Fig. 19 (a, b) Open-circuit voltage for 0.9 g CSE + 1 g PVA + 0.45wt% $MgCl_2$

Appendix

Figure 20.

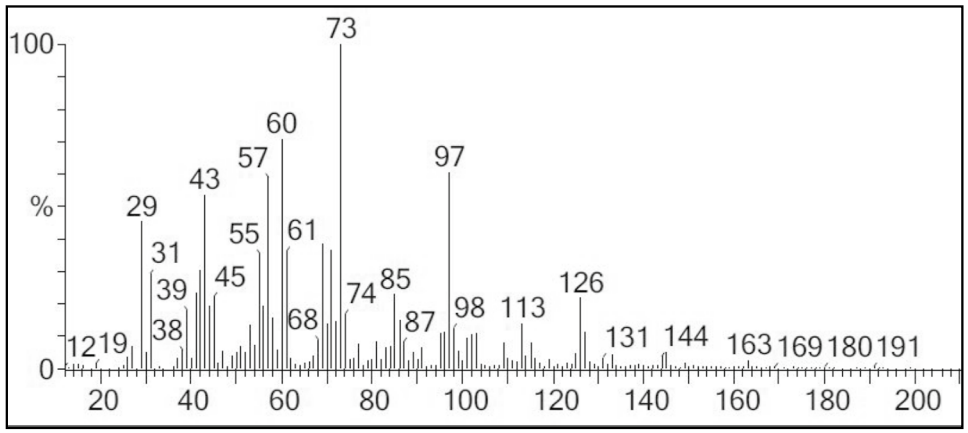

Chromatogram of Melezitose

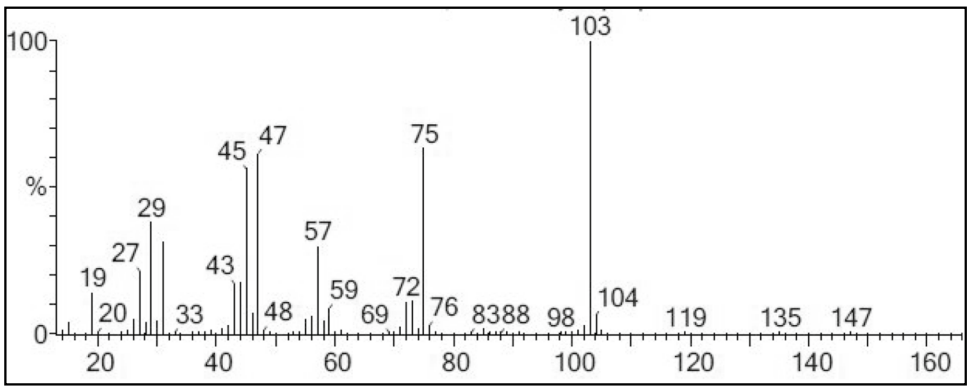

Chromatogram of 3,3-diethoxy 1-propanol

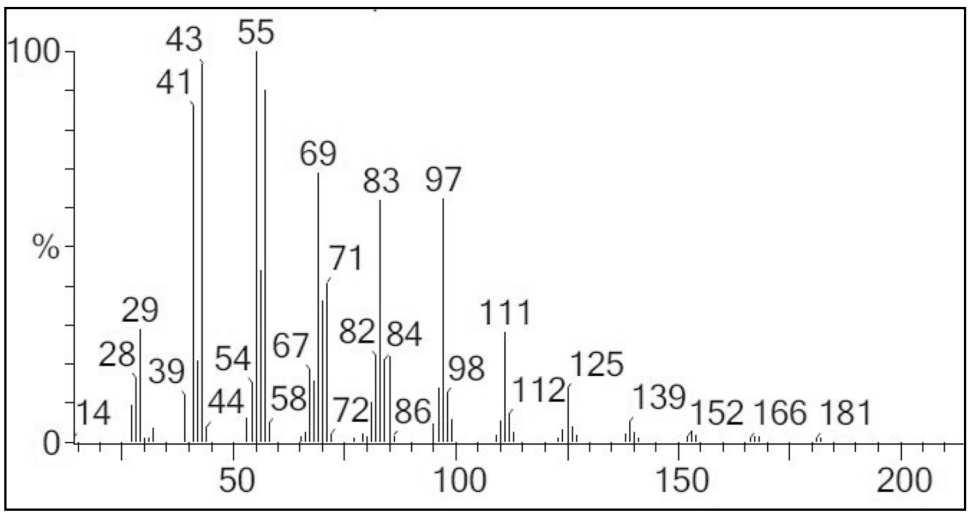

Chromatogram of 1-docosene

Fig. 20 GC–MS chromatogram of the compounds in corn silk extract

Fig. 20 (continued)

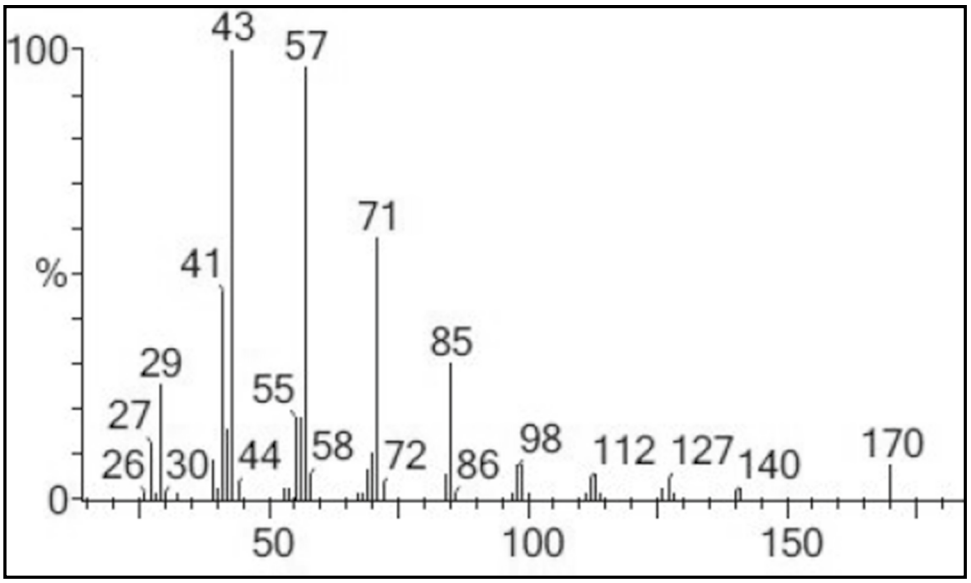

Chromatogram of dodecane

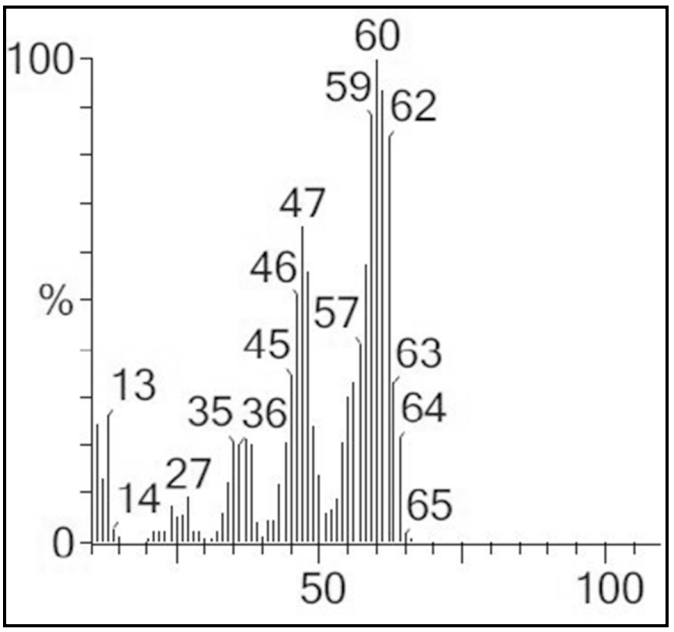

Chromatogram of pentaborane

Funding One of the authors Dr. S. Jone Kirubavathy would like to thank GRG Trust, Coimbatore, India, for their financial support.

References

1. Perumal P, Christopher Selvin P, Selvasekarapandian S (2018) Characterization of biopolymer pectin with lithium chloride and its applications to electrochemical devices. Ionics 24:3259–3270. https://doi.org/10.1007/s11581-018-2507-5
2. Muthukrishnan M, Shanthi C, Selvasekarapandian S et al (2019) Synthesis and characterization of pectin-based biopolymer electrolyte for electrochemical applications. Ionics 25:203–214. https://doi.org/10.1007/s11581-018-2568-5
3. Selvalakshmi S, Mathavan T, Selvasekarapandian S, Premalatha M (2017) Study on NH4I composition effect in agar–agar-based biopolymer electrolyte. Ionics 23:2791–2797. https://doi.org/10.1007/s11581-016-1952-2
4. Boopathi G, Pugalendhi S, Selvasekarapandian S et al (2017) Development of proton conducting biopolymer membrane based on agar–agar for fuel cell. Ionics 23:2781–2790. https://doi.org/10.1007/s11581-016-1876-x
5. Nirmala Devi G, Chitra S, Selvasekarapandian S et al (2017) Synthesis and characterization of dextrin-based polymer electrolytes for potential applications in energy storage devices. Ionics 23:3377–3388. https://doi.org/10.1007/s11581-017-2135-5
6. Monisha S, Mathavan T, Selvasekarapandian S et al (2017) Investigation of bio polymer electrolyte based on cellulose acetate-ammonium nitrate for potential use in electrochemical devices. Carbohyd Polym 157:38–47. https://doi.org/10.1016/j.carbpol.2016.09.026
7. Monisha S, Selvasekarapandian S, Mathavan T et al (2016) Preparation and characterization of biopolymer electrolyte based on cellulose acetate for potential applications in energy storage devices. J Mater Sci: Mater Electron 27:9314–9324. https://doi.org/10.1007/s10854-016-4971-x
8. Parsimehr H, Ehsani A (2020) Corn-based electrochemical energy storage devices. Chem Rec 20:1163–1180
9. Rani MSA, Rudhziah S, Ahmad A, Mohamed NS (2014) Biopolymer electrolyte based on derivatives of cellulose from kenaf bast fiber. Polymers 6:2371–2385. https://doi.org/10.3390/polym6092371
10. Pan Y, Wang C, Chen Z et al (2017) Physicochemical properties and antidiabetic effects of a polysaccharide from corn silk in high-fat diet and streptozotocin-induced diabetic mice. Carbohyd Polym 164:370–378. https://doi.org/10.1016/j.carbpol.2017.01.092
11. Guo Q, Xu L, Chen Y et al (2019) Structural characterization of corn silk polysaccharides and its effect in H2O2 induced oxidative damage in L6 skeletal muscle cells. Carbohyd Polym 208:161–167. https://doi.org/10.1016/j.carbpol.2018.12.049
12. Ali GW, Abdel-Fattah WI, Elhaes H, Ibrahim MA (2019) Spectroscopic and modeling analyses of bimolecular structure of corn silk. Biointerface Res Appl Chem 9:4581–4585. https://doi.org/10.33263/BRIAC96.581585
13. Hasanudin K, Hashim P, Mustafa S (2012) Corn silk (Stigma Maydis) in healthcare: a phytochemical and pharmacological review. Molecules 17:9697–9715
14. Limmatvapirat C, Nateesathittarn C, Dechasathian K et al (2020) Phytochemical analysis of baby corn silk extracts. J Ayurveda Integr Med 11:344–351. https://doi.org/10.1016/j.jaim.2019.10.005
15. Chen S, Chen H, Tian J et al (2013) Chemical modification, antioxidant and α-amylase inhibitory activities of corn silk polysaccharides. Carbohyd Polym 98:428–437. https://doi.org/10.1016/j.carbpol.2013.06.011
16. Liu J, Wang C, Zhang T et al (2011) Subchronic toxicity study of corn silk with rats. J Ethnopharmacol 137:36–43. https://doi.org/10.1016/j.jep.2011.03.021
17. Jayaram S, Kapoor S, Dharmesh SM (2015) Pectic polysaccharide from corn (Zea mays L.) effectively inhibited multi-step mediated cancer cell growth and metastasis. Chem Biol Interact 235:63–75. https://doi.org/10.1016/j.cbi.2015.04.008
18. Liew CW, Ramesh S (2015) Electrical, structural, thermal and electrochemical properties of corn starch-based biopolymer electrolytes. Carbohyd Polym 124:222–228. https://doi.org/10.1016/j.carbpol.2015.02.024
19. Vadivazhagan M, Parameswaran P, Mani U, Nallathamby K (2018) Waste-driven bio-carbon electrode material for Na-ion storage applications. ACS Sustain Chem Eng 6:13915–13923. https://doi.org/10.1021/acssuschemeng.8b02199
20. Wan W, Wang Q, Zhang L et al (2016) N-, P- and Fe-tridoped nanoporous carbon derived from plant biomass: an excellent oxygen reduction electrocatalyst for zinc-air batteries. J Mater Chem A 4:8602–8609. https://doi.org/10.1039/c6ta02150f
21. Kim HS, Arthur TS, Allred GD, et al (2011) Structure and compatibility of a magnesium electrolyte with a sulphur cathode. Nat Commun 2. https://doi.org/10.1038/ncomms1435
22. Hamsan MH, Aziz SB, Kadir MFZ, et al (2020) The study of EDLC device fabricated from plasticized magnesium ion conducting chitosan based polymer electrolyte. Polym Test 90. https://doi.org/10.1016/j.polymertesting.2020.106714
23. Manjuladevi R, Thamilselvan M, Selvasekarapandian S et al (2017) Mg-ion conducting blend polymer electrolyte based on poly(vinyl alcohol)-poly (acrylonitrile) with magnesium perchlorate. Solid State Ion 308:90–100. https://doi.org/10.1016/j.ssi.2017.06.002
24. Sangeetha P, Selvakumari TM, Selvasekarapandian S et al (2020) Preparation and characterization of biopolymer K-carrageenan with MgCl2 and its application to electrochemical devices. Ionics 26:233–244. https://doi.org/10.1007/s11581-019-03193-0
25. Hamsan MH, Aziz SB, Nofal MM et al (2020) Characteristics of EDLC device fabricated from plasticized chitosan:MgCl2 based polymer electrolyte. J Market Res 9:10635–10646. https://doi.org/10.1016/j.jmrt.2020.07.096
26. Mahalakshmi M, Selvanayagam S, Selvasekarapandian S et al (2019) Characterization of biopolymer electrolytes based on cellulose acetate with magnesium perchlorate (Mg(ClO4)2) for energy storage devices. J Sci Adv Mater Dev 4:276–284. https://doi.org/10.1016/j.jsamd.2019.04.006
27. Perumal P, Abhilash KP, P.Sivaraj, Selvin PC (2019) Study on Mg-ion conducting solid biopolymer electrolytes based on tamarind seed polysaccharide for magnesium ion batteries. Mater Res Bullet 118. https://doi.org/10.1016/j.materresbull.2019.05.015
28. Parameswaran V, Nallamuthu N, Devendran P et al (2017) Electrical conductivity studies on Ammonium bromide incorporated with Zwitterionic polymer blend electrolyte for battery application. Physica B 515:89–98. https://doi.org/10.1016/j.physb.2017.03.043
29. Pandi DV, Selvasekarapandian S, Bhuvaneswari R et al (2016) Development and characterization of proton conducting polymer electrolyte based on PVA, amino acid glycine and NH4SCN. Solid State Ion 298:15–22. https://doi.org/10.1016/j.ssi.2016.10.016
30. Reddy TJR, Achari VBS, Sharma AK, Rao VVRN (2007) Effect of plasticizer on electrical conductivity and cell parameters of (PVC+KBr O3) polymer electrolyte system. Ionics 13:55–59. https://doi.org/10.1007/s11581-007-0072-4
31. Polu AR, Kumar R (2013) Preparation and characterization of pva based solid polymer electrolytes for electrochemical cell

applications. Chin J Polym Sci (English Edition) 31:641–648. https://doi.org/10.1007/s10118-013-1246-3
32. Oliveira RN, Mancini MC, de Oliveira FCS et al (2016) Análise por FTIR e quantificação de fenóis e flavonóides de cinco produtos naturais disponíveis comercialmente utilizados no tratamento de feridas. Revista Materia 21:767–779. https://doi.org/10.1590/S1517-707620160003.0072
33. Mansur HS, Sadahira CM, Souza AN, Mansur AAP (2008) FTIR spectroscopy characterization of poly (vinyl alcohol) hydrogel with different hydrolysis degree and chemically crosslinked with glutaraldehyde. Mater Sci Eng C 28:539–548. https://doi.org/10.1016/j.msec.2007.10.088
34. Rajeswari N, Selvasekarapandian S, Prabu M et al (2013) Lithium ion conducting solid polymer blend electrolyte based on biodegradable polymers. https://doi.org/10.1007/s12034-013-0463-2
35. Aziz SB, Dannoun EMA, Hamsan MH, et al (2021) Improving edlc device performance constructed from plasticized magnesium ion conducting chitosan based polymer electrolytes via metal complex dispersion. Membranes 11. https://doi.org/10.3390/membranes11040289
36. Evans J, Vincent CA, Bruce PG Electrochemical measurement of transference numbers in polymer electrolytes
37. Shanmuga Priya S, Karthika M, Selvasekarapandian S, Manjuladevi R (2018) Preparation and characterization of polymer electrolyte based on biopolymer I-Carrageenan with magnesium nitrate. Solid State Ion 327:136–149. https://doi.org/10.1016/j.ssi.2018.10.031
38. Ramaswamy M, Malayandi T, Subramanian S et al (2017) Magnesium ion conducting polyvinyl alcohol–polyvinyl pyrrolidone-based blend polymer electrolyte. Ionics 23:1771–1781. https://doi.org/10.1007/s11581-017-2023-z
39. Mishra R, Baskaran N, Ramakrishnan PA, Rao KJ (1998) Lithium ion conduction in extreme polymer in salt regime
40. Boukamp BA (1986) A package for impedance/admittance data analysis
41. Boukamp BA A nonlinear least squares fit procedure for analysis of immittance data of electrochemical systems
42. Ramya CS, Selvasekarapandian S, Savitha T et al (2006) Conductivity and thermal behavior of proton conducting polymer electrolyte based on poly (N-vinyl pyrrolidone). Eur Polymer J 42:2672–2677. https://doi.org/10.1016/j.eurpolymj.2006.05.020
43. Chandra MVL, Karthikeyan S, Selvasekarapandian S et al (2017) Study of PVAc-PMMA-LiCl polymer blend electrolyte and the effect of plasticizer ethylene carbonate and nanofiller titania on PVAc-PMMA-LiCl polymer blend electrolyte. J Polym Eng 37:617–631. https://doi.org/10.1515/polyeng-2016-0145
44. Kiruthika S, Malathi M, Selvasekarapandian S et al (2020) Conducting biopolymer electrolyte based on pectin with magnesium chloride salt for magnesium battery application. Polym Bull 77:6299–6317. https://doi.org/10.1007/s00289-019-03071-9